



Kent Academic Repository

Honeybone, P.J.R., Newport, R.J., Howells, W.S. and Franks, J. (1990) *The Structure of a-C:H Thin Films*. In: Clausing, R.E. and Horton, L.L. and Angus, J.C. and Koidl, P., eds. *Diamond and Diamond-like Films and Coatings*. NATO ASI Series . Springer, Boston, Massachusetts, USA, pp. 321-329. ISBN 978-1-4684-5969-2.

Downloaded from

<https://kar.kent.ac.uk/15906/> The University of Kent's Academic Repository KAR

The version of record is available from

https://doi.org/10.1007/978-1-4684-5967-8_20

This document version

Publisher pdf

DOI for this version

Licence for this version

UNSPECIFIED

Additional information

Conference Information: NATO ADVANCED STUDY INST ON DIAMOND AND DIAMOND-LIKE FILMS AND COATINGS CASTELVECCHIO ITALY, JUL 22-AUG 03, 1990 NATO, DIV SCI AFFAIRS; OAK RIDGE NATL LAB, MET & CERAM DIV; FRAUNHOFER INST ANGEW FESTKORPERPHYS; NATL SCI FDN; CONSORZLO INST NAZL FIS MAT; USN, OFF NAVAL RES; NANO INSTRUMENTS; USA, EUROPEAN RES OFF; APPL SCI & TECHNOL; POLITEC TORINO Source: DIAMOND AND DIAMOND-LIKE FILMS AND COATINGS Book Series: NATO ADVANCED SCIENCE INSTITUTES SERIES, SERIES B, PHYSICS ISBN: 0-306-44004-0

Versions of research works

Versions of Record

If this version is the version of record, it is the same as the published version available on the publisher's web site. Cite as the published version.

Author Accepted Manuscripts

If this document is identified as the Author Accepted Manuscript it is the version after peer review but before type setting, copy editing or publisher branding. Cite as Surname, Initial. (Year) 'Title of article'. To be published in *Title of Journal*, Volume and issue numbers [peer-reviewed accepted version]. Available at: DOI or URL (Accessed: date).

Enquiries

If you have questions about this document contact ResearchSupport@kent.ac.uk. Please include the URL of the record in KAR. If you believe that your, or a third party's rights have been compromised through this document please see our [Take Down policy](https://www.kent.ac.uk/guides/kar-the-kent-academic-repository#policies) (available from <https://www.kent.ac.uk/guides/kar-the-kent-academic-repository#policies>).

THE STRUCTURE OF a-C:H THIN FILMS

P.J.R. Honeybone and R.J. Newport
Physics Laboratory, The University of Canterbury
Caonterbury, Kent

P.J.R. Honeybone and R.J. Newport
Physics Laboratory, The University of Canterbury
Kent, CT2 7NR UK

W.S. Howells
Neutron Scince Division
Rutherford Appelton Laboratory
Chilton, Didcot, Oxon OX11 0QX UK

J. Franks
Ion Tech Ltd.
2 Park Street
Teddington, Middx. TW11 0Lt UK

INTRODUCTION

The structure of amorphous hydrogenated carbon (a-C:H), prepared under certain conditions, is such that it is harder, denser and more resistant to chemical attack than any other solid hydrocarbon. This, coupled with its high infra-red transparency and the ability to control the as-deposited properties to suit specific requirements, has led to many applications [1].

The material is thought to consist of clusters of sp^2 hybridised carbon interconnected by regions of sp^3 carbon in a continuous random network, with the $sp^2:sp^3$ ratio varying between 1:2 to 2:1, depending on exact deposition conditions. The high degree of sp^2 clustering suggested by optical gap measurements indicates that intermediate, as well as short range order, are important. The reviews by Angus et al [2] and Robertson [3] provide an excellent outline of this and other model structures.

There have been few direct diffraction experiments performed on a-C:H and these have been limited mainly to electron diffraction (e.g. McKenzie et al. [4]) in which the K-space range of available data is too restricted to extract high resolution real-space information. Neutron diffraction, especially from a pulsed source, overcomes this resolution problem by taking a significantly wider data range than is possible by electron or X-ray diffraction. Neutron diffraction also probes the hydrogen environment in a direct way.

Complementary information concerning the local bonding configurations can be obtained from the vibrational properties of the material. Optical probes (IR and Raman spectroscopy) have been widely used in this way, and comprehensive tables have been published [7]. The incoherent neutron scattering cross-section of hydrogen is several orders of magnitude greater than that for carbon. Incoherent inelastic neutron scattering takes advantage of this with the effect that the observed spectra are, to a very good approximation, purely from the hydrogen vibrations.

EXPERIMENTAL DETAILS

The amorphous hydrogenated carbon used in these experiments was produced using a saddle field ion beam source [6]. Samples 1 and 2 (prepared from propane and acetylene gases respectively) were deposited in the conventional way onto copper substrates (- as a-C:H does not adhere to copper, this proved an ideal method for providing the large, ~ 2-5 gm, powder samples required for neutron scattering experiments). Sample 3 was collected from within the source chamber and had been deposited over a period of time, from a mixture of propane, butane and acetylene gases.

The neutron diffraction and inelastic neutron scattering data were collected at the ISIS pulsed neutron source (Rutherford Appleton Laboratory) using the LAD diffractometer and the TFXA spectrometer respectively (see Figure 2; detailed information can be found elsewhere [7]). The analysis of the neutron diffraction data is only fully complete for samples 1 and 3.

A spallation neutron source, such as the one at the Rutherford Appleton Laboratory produces a pulse of neutrons with a spread of velocities, and thus a spread of arrival times at any one detector. This gives a smooth variation of neutron wavelength as a function of time-of-flight ($\lambda \approx t/l$ where t is the time-of-flight over path length l)

The LAD detectors are arranged so that, on each side of the instrument there were detectors at fixed scattering angles. Spectra were recorded separately, as a function of time-of-flight, for each of these detector pairs and also for monitors in the incident and in the transmitted beam. Spectra were recorded for each of the samples together with their respective empty containers, the no-sample background and for a vanadium rod. The vanadium rod is used as a "standard" and provides the information necessary to put the sample scattering on absolute scale [8]. TFXA uses a time-focussed pyrolytic graphite crystal analyser to resolve the scattered beam, with an extended detector array covering 0.06 steradians.

A Carlo Erba CHN combustion analyser was used to determine the compositions of the samples. Infra-red measurements were performed using a Mattson Instruments Alpha Centauri FTIR and densities were determined using a residual volume technique.

Table 1. Compositions and densities of samples

		C (at.%)	H (at.%)	ρ (g cm ⁻³)	ρ_N (gram atom cm ⁻³)
Sample 1	Propane	0.68	0.32	1.66	0.20
Sample 2	Acetylene	0.65	0.35	1.51	0.19
Sample 3	Mixture	0.71	0.29	1.65	0.19

THEORETICAL BACKGROUND

The object of performing a diffraction experiment is to determine the structure factor, $S(Q)$ where, for an amorphous material (i.e. an isotropic scatterer) [8]:

$$S(Q) = 1 + 4\pi\rho/Q \int_0^{\infty} r dr (g(r) - 1) \sin(Qr) \quad (1)$$

where ρ is the average number density of atoms in the material, Q is the wave vector transfer associated with the diffraction experiment - which for a liquid or amorphous solid, is defined as $Q = 4\pi \sin \theta/\lambda$ where 2θ is the scattering angle - and $g(r)$ is the pair correlation function, which is a measure of the atomic density at a distance r from a given atom at the origin. The pair correlation function may therefore be obtained by Fourier transformation of the structure factor.

In a multi-component system, there are contributions to the total structure factor from each atom-type pair. For a binary alloy a-C:H this yields three terms, which are weighted thus to give a total structure factor, $F(Q)$:

$$F(Q) = \sum_{\alpha} c_{\alpha} b_{\alpha}^2 + \sum_{\alpha, \beta} c_{\alpha} b_{\alpha} c_{\beta} b_{\beta} S_{\alpha\beta}(Q) - 1 \quad (2)$$

where c_{α} is the atomic fraction, and b_{α} the coherent scattering length respectively of element α . The first summation represents the "self" or "single atom" scattering while the second is the "interference" or "distinct" scattering term and contains the basic information on atomic positions. A Fourier transformation of $S_{\alpha\beta}(Q)$ leads to the total radial distribution function, $G(r) = \sum_{\alpha\beta} [c_{\alpha} c_{\beta} b_{\alpha} b_{\beta} g_{\alpha\beta}(r)]$ where the $g_{\alpha\beta}(r)$ represent the partial terms in $G(r)$. Weightings of individual terms in the structure factor and radial distribution are displayed in Table 2. (It should be noted that the C-H partial term is equivalent to the H-C term). It can be seen that the C-C and C-H terms will dominate the $F(Q)$ and $G(r)$.

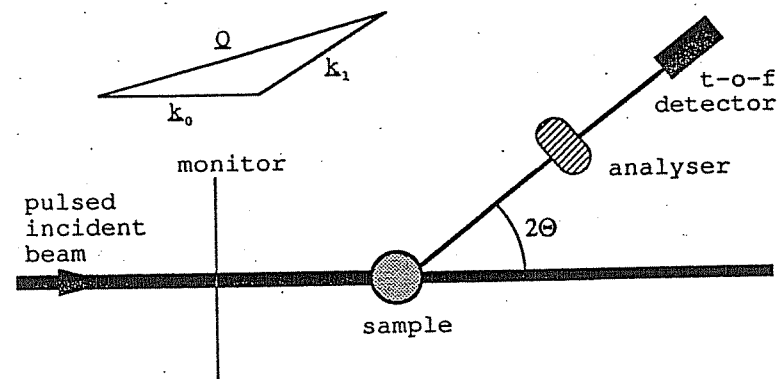


Figure 1. Schematic diagram of neutron scattering instruments. (The analyser crystal is absent in the diffraction case) With inset scattering triangle.

Table 2. Partial Contributions to F(Q) and G(r)

Term	C-C	C-H	H-H
Sample 1	20.4	-5.4	1.4
Sample 3	22.3	-5.1	1.2

A neutron interacting with matter transfers energy, as well as momentum to the system. This results in the need for a detailed inelasticity correction for neutron diffraction experiments, but provides the basis for inelastic neutron scattering experiments in which the energy transfer, $\hbar\omega$, as well as Q is measured (- in the case of TFXA this is achieved by determining the energy of the scattered neutrons using a crystal analyser). Given hydrogen's large cross-section for incoherent scattering, which dominates the total scattering cross-section for these samples (see Table 3), the measured scattering from TFXA is, to a very good approximation, given by the incoherent term. In this situation, the scattering function can be related directly to the vibrational density of states, $g(\omega)$. A fuller description of inelastic scattering theory can be found elsewhere [9,10].

DATA ANALYSIS

Each of the diffraction data sets is in the form of a number of spectra, one for each detector, consisting of counts as a function of time-of-flight. Before obtaining the F(Q) several corrections need to be applied, full details of which can be found elsewhere [11]. The major corrections are for background, container and multiple scattering, attenuation and the effects of inelasticity. The vanadium is used to put the sample scattering on an absolute scale.

In hydrogenous materials, the inelasticity correction is in many ways the most problematic step in the correction procedures. The simplistic approaches to the problem [12] break down for low atomic mass systems, and alternative routes need to be adopted. Jung et al. [13] suggested a semi-empirical technique for their work on methylene chloride which is based on estimating an effective average molecular mass. The principal elements of their approach are used here to provide a model for the effects of inelasticity.

RESULTS

Angus et al [2] suggest that, for a hard carbon film, a gram atom density greater than 0.2 is required, with lower densities corresponding to a softer, more polymeric structure. This indicates that these samples are intermediate between the soft and hard a-C:H. Confirmation of this can be found from analysis of the C-H stretch, which indicates the presence of small quantities of CH₃ and olefinic CH₂ groups, which only appear in the polymeric films.

Examination of the radial distribution function G(r) from sample 1 (see figure 2b) reveals a split C-C peak at 1.39 and 1.52 ± 0.02Å. Comparison of the peak positions with known C-C bond lengths (see table 3) shows that the 1.52Å peak is unambiguously the single bond length and that the 1.39Å bond length

Table 3. Bond Lengths of Carbon and Hydrogen

C-C	Diamond	1.54Å
C-C	Graphite	1.42Å
C-C	Benzene	1.3954Å
C-C	Ethene	1.34Å
C-H	Methane	1.094Å
C-H	Ethene	1.074Å
H-H	Hydrogen	0.754Å

corresponds closest to that found in aromatic compounds, by contributions from the 1.52Å peak. The ratio 1.39Å : 1.52Å bonds has been found to be 1:4 and the average number of carbon atoms bonded to each carbon atom is estimated to be about 2.5 (the exact uncertainty is unknown, but it is expected to be quite large). The ratio of sp²:sp³ carbon is unknown, although the predominance of σ-bonding and the relatively high average C-C coordination both suggest a high sp³ concentration.

The other features in the G(r) can be ascribed to a C-H bond (1.07Å), with a coordination number of 1.0 (due to the close proximity of all C-H bond distances it is not possible to identify the dominant hydrogen location), an H-H peak at 0.8Å which is either molecular hydrogen or H-H distances between neighbouring CH_n groups (it is hoped that molecular modelling will cast more light on this in the near future).

Moving beyond the first coordination shell, the broad feature between 2.3 and 2.7Å is a combination of sp² and sp³ C-C-C distances, with an average carbon coordination number of 4.0. Resolving the individual contributions is not possible because of the proximity of the two distances, and the likely spread of these distances as bond angles vary between local configurations.

Preliminary analysis of the diffraction data from sample 2 shows that the structure factor is very similar to that of sample 1. The only difference seems to be at low Q, which would correspond to differences in the intermediate range order in the continuous random network. A full analysis of this system should be completed in the near future.

Comparison of the structure factors from samples 1 and 3 shows that it is only at low Q that the structure differs. This would suggest that the structure is very similar for the samples prepared in different parts of the vacuum chamber. Studying the radial distribution functions, again, many similarities are evident; both samples have the same C-H and first and second shell C-C coordination, numbers and have a feature at low r (< 1Å) which corresponds to a H-H distance.

The inelastic data confirms that there is very little difference in the vibrational structures of the three samples (see figure 3), with the three spectra being equivalent (to within experimental error) for frequencies in the 200 to 4000 cm⁻¹ range. Within this range, there are clear peaks at ~870cm⁻¹, 1250cm⁻¹ and 3000cm⁻¹. Comparison with published IR work [5] shows that all three vibrations are consistent with olefinic C-H

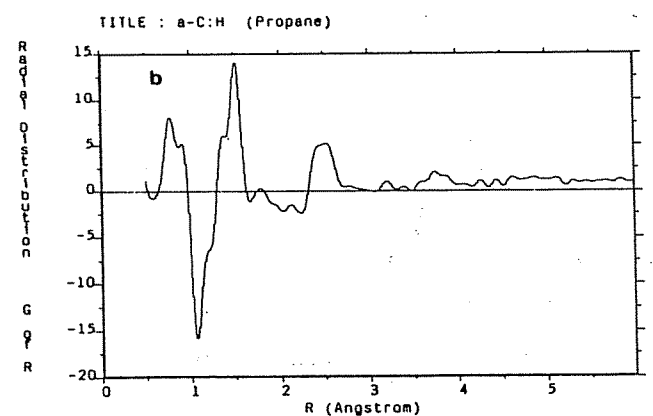
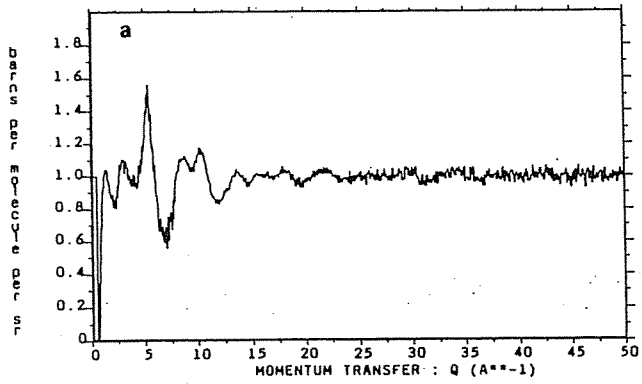


Figure 2. (a) S(Q) and (b) G(r) for sample 1

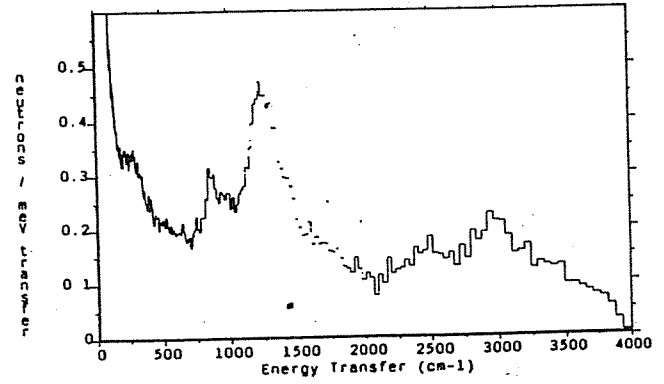


Figure 3. IINS spectrum for Sample 1

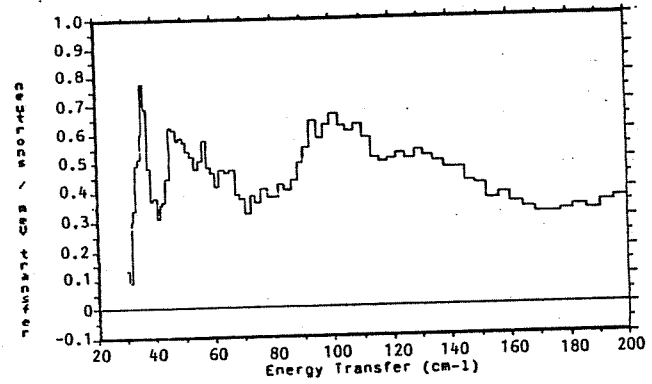


Figure 4. IINS spectrum for sample 3 in the 30-200 $\bar{c}m^{-1}$ range

group vibrations, although the poor resolution at $\sim 3000\text{cm}^{-1}$ precludes any definitive assignment of this vibration. Although the olefinic C-H groups dominate the inelastic spectrum, there are signs that small contributions are made by other CH_3 groups, giving a general background to the $600\text{--}1800\text{cm}^{-1}$ region. The inelastic data seems to contrast with NMR work [14] which shows preferential bonding of hydrogen to sp^3 sites. Further work is required to clarify the situation.

The differences that occur between both conventionally prepared samples (samples 1 and 2) are at very low energy ($\omega < 120\text{ cm}^{-1}$) (see figure 4). The modes giving rise to this are seen in both samples, but with more intensity in sample 1 than in sample 2. These have been tentatively assigned to oscillations of relatively large regions of the continuous random network, and would be consistent with torsions of extended graphitic regions.

A surprising feature is the presence of molecular hydrogen in sample 3. Its presence in amorphous hydrogenated solids has previously been indicated by many techniques (e.g., IR on a-Si:H by Chabal and Patel [15]) but never before seen directly with neutrons. In a linear molecule, such as molecular hydrogen, the rotational energy levels are given by [16]:

$$E_J = hcBJ(J + 1) \quad (3)$$

where E_J is the energy of the J^{th} rotational level, and $B = \hbar^2/4\pi cI$, with I being the moment of inertia. Thus, the transition from the $J = 0$ to $J = 1$ energy levels requires $2hcB\text{ cm}^{-1}$. The rotation for molecular hydrogen can be seen at $\sim 110\text{cm}^{-1}$. This can be used to determine the moment of inertia, and hence the bond length. This method was used to determine the hydrogen bond length, which was found to be $\sim 0.72\text{ \AA}$, c.f. the accepted value of 0.75 \AA for free hydrogen and 0.65 \AA as determined by diffraction. The splitting of the INS band is indicative of asymmetry in the hydrogen environment, resulting in the hydrogen molecules being contained within oblate or prolate spheroids.

CONCLUSIONS

The three samples are all intermediate between soft and hard a-C:H and show little if any difference in their short range order, although there is evidence of differences in the intermediate range order. This is likely to be due to the graphitic regions varying in size and/or number from sample to sample.

From the diffraction data it can be deduced that the single bonds form the bulk of the random network, with a smaller, but nonetheless significant proportion of double or aromatic bonds. This data also shows that bonded hydrogen dominates over free hydrogen, although small quantities of molecular hydrogen have been detected in one sample by IINS.

The inelastic experiment, in particular, probed the hydrogen environment. This data suggests that hydrogen is bonded mainly at olefinic carbon sites, with smaller amounts at other sites. Also, molecular hydrogen has been discovered in one sample, although the quantity is small. Hopefully, molecular modelling

of the diffraction data, which is now in progress using a Monte-Carlo based technique [19], will yield more information.

There remain many unanswered questions concerning the structure of a-C:H. Clarification of the hydrogen bonding environment is required and questions remain concerning the nature and extent sp^2 and sp^3 of regions. Further work using neutron and synchrotron X-ray techniques together with computer modelling is in progress which will address these outstanding issues.

ACKNOWLEDGEMENTS

We would like to thank Mr. A. Evans and Dr. P.J. Revell of Ion Tech Ltd., for their help in depositing the a-C:H, Mr. A. Fassam (Chemistry Department, UKC) for his help in determining the compositions and members of the Kent group for helpful discussions. One of us (PJRH) acknowledges the receipt of a SERC studentship.

REFERENCES

1. A.H. Lettington, "Amorphous Hydrogenated Carbon Films", E-MRS Proceedings, 17 P. Koidl and P. Oelhafen, eds. (1987).
2. J.C. Angus, P. Koidl, and S. Domitz, Chapter 4 in: "Plasma deposited thin films", J. Mort and F. Jansen, eds., CRC Press, Boca Raton (1986).
3. J. Robertson, Advances in Physics, 35 317 (1986).
4. D.R. McKenzie, L.C. Botten, and R.C. McPhedran, Physics Review Letters, 51 280 (1983).
5. B. Dischler, "Amorphous Hydrogenated Carbon Films", E-MRS Proceedings, 17 P. Koidl and P. Oelhafen, eds. (1987).
6. J. Franks, Vacuum, 34 259 (1984).
7. ISIS Annual Report 1989, Rutherford Appleton Laboratory Report RAL-89-050.
8. R.J. Newport, Chapter 13 in "Neutron Scattering at a Pulsed Source", R.J. Newport, B.D. Rainford and R. Cywinski, eds., Adam Hilger, Bristol, (1988).
9. R.N. Sinclair, J. of Non-Cryst., So., 76 61, (1985).
10. J. Tomkinson, Chapter 18 in "Neutron Scattering at a Pulsed Source", R.J. Newport, B.D. Rainford and R. Cywinski, eds., Adam Hilger, Bristol, (1988).
11. A.K. Soper, W.S. Howells and A.C. Hannon, ATLAS - Analysis of time-of-flight diffraction data from liquid and amorphous samples, Rutherford Appleton Laboratory, Report RAL-89-046, (1989).
12. G. Placzek, Physical Review, 86 377, 1952.
13. W.G. Jung, M.D. Zeidler and P. Chieux, Mol. Phys., 68 473 (1989).
14. M.A. Petrich, Materials Science forum, 52 377 (1989).
15. J. Howard, C.J. Ludman and J. Tomkinson, Fuel, 62 1097 (1983).
16. P.W. Atkins, Physical Chemistry, OUP, Oxford (1978).
17. Y.J. Chabal and C.K.N. Patel, Phys. Rev. Letts., 53 210 (1984).
18. R.L. McGreevy and L. Putsztai, Mol. Simulation, 1 359 (1988).